

Supplementary Information

Uniform self-rectifying resistive random access memory based on MXene-TiO₂

Schottky junction

Chao Zang^{1,2#}, Bo Li^{1,2#}, Yun Sun^{1*}, Shun Feng^{1,3}, Xin-Zhe Wang^{1,2}, Xiaohui Wang^{1,2*},

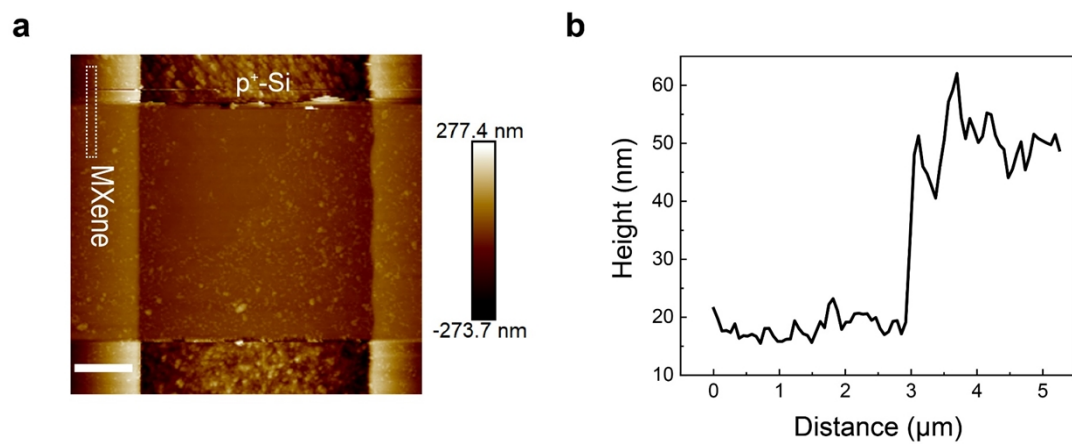
Dong-Ming Sun^{1,2*}

¹Shenyang National Laboratory for Materials Science, Institute of Metal Research,
Chinese Academy of Sciences, 72 Wenhua Road, Shenyang, 110016, China.

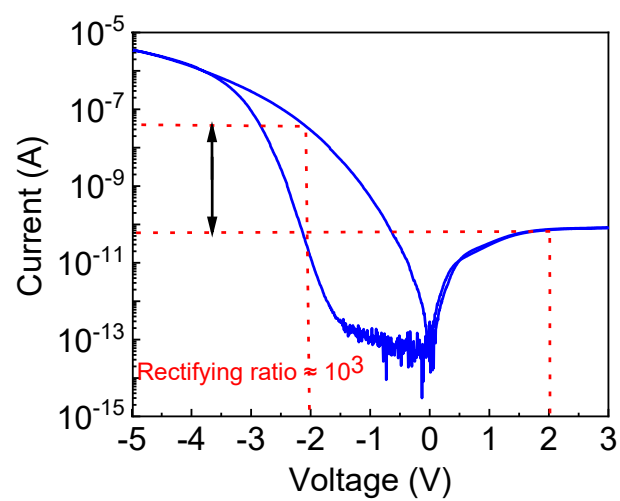
²School of Material Science and Engineering, University of Science and Technology of
China, 72 Wenhua Road, Shenyang, 110016, China.

³School of Physical Science and Technology, ShanghaiTech University, 393
Huaxiazhong Road, Shanghai, 200031, China.

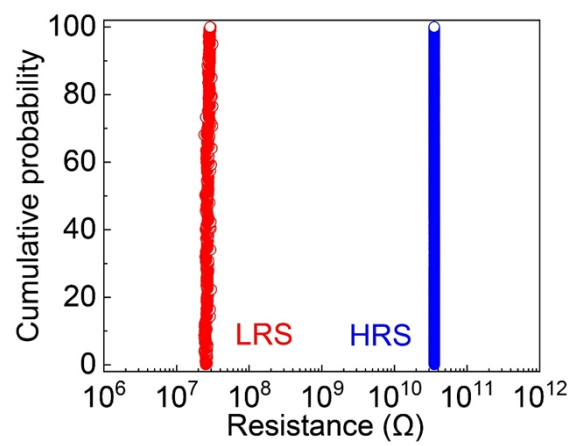
[#]These authors were equal major contributors to this work.



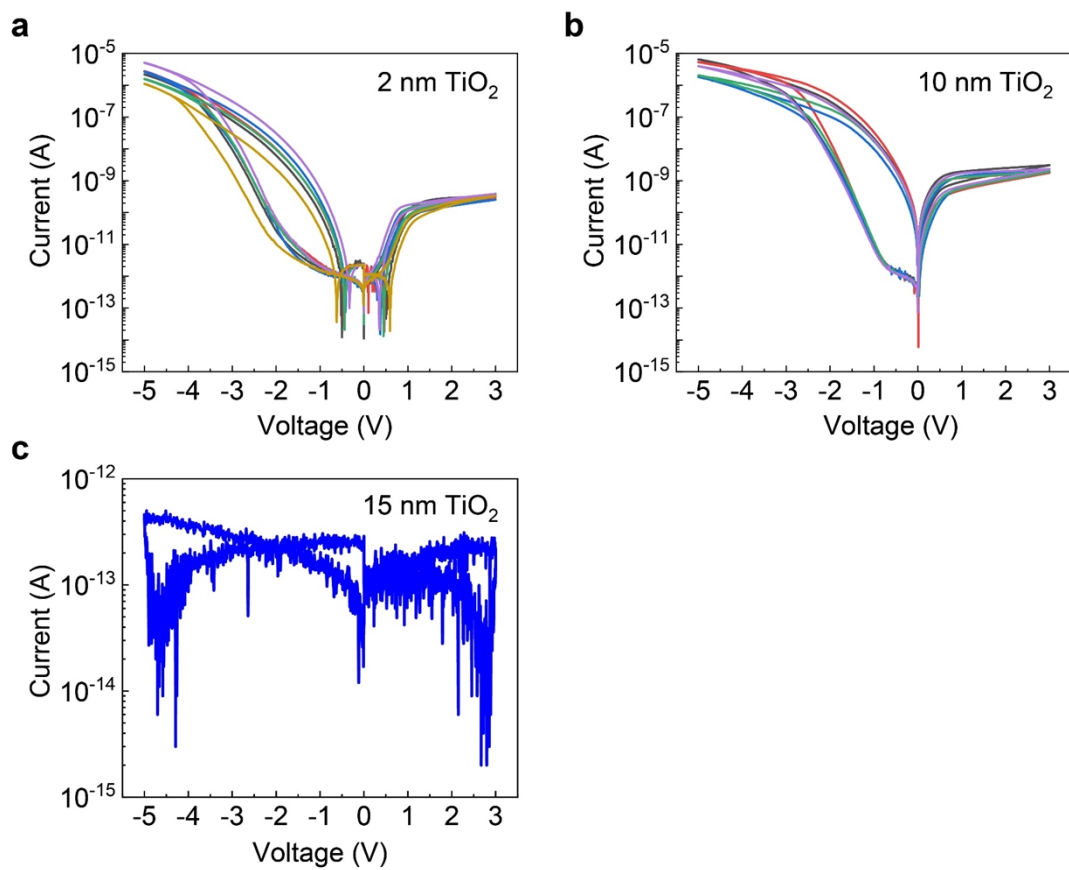
Supplementary Fig. 1 (a) AFM image of the morphology of MXene film. Scale bar, 2 μm . (b) Height profile along the white dashed line in (a), indicating a thickness of 25 nm MXene.



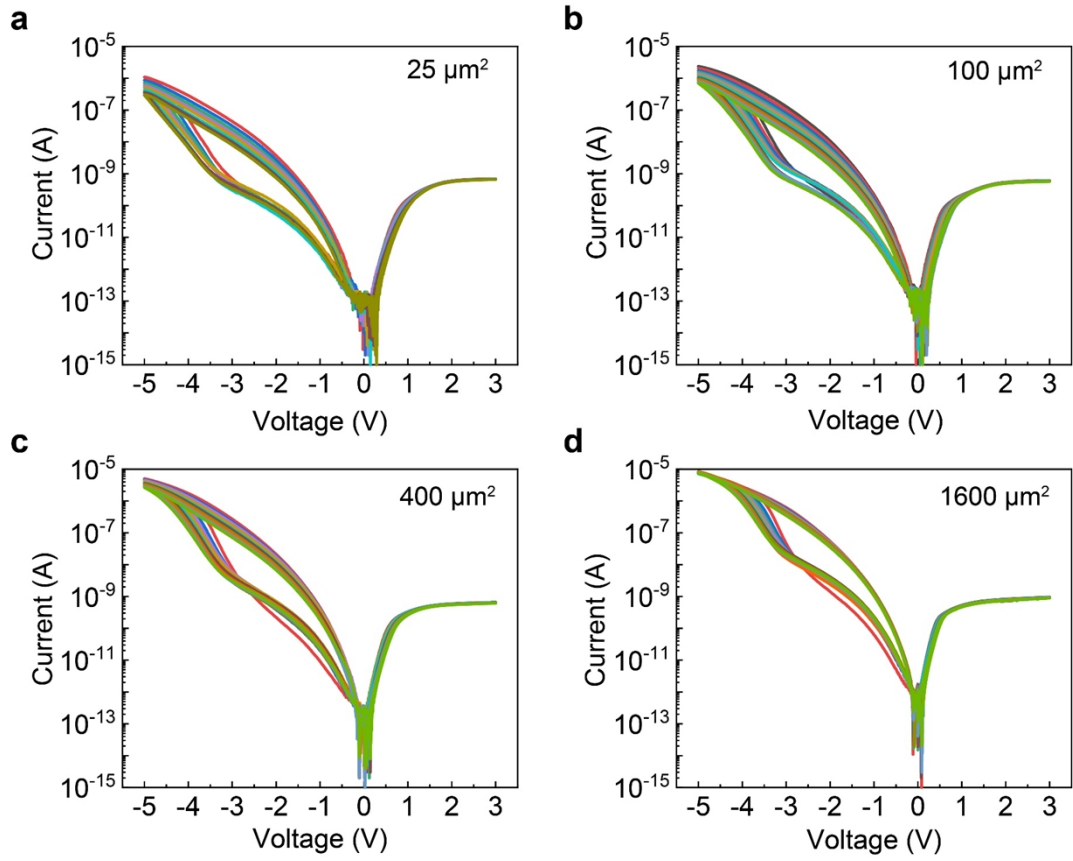
Supplementary Fig. 2 Typical I - V characteristic of an MXene-TiO₂-Si RRAM with a rectifying ratio of 10^3 obtained at 2 V and -2 V.



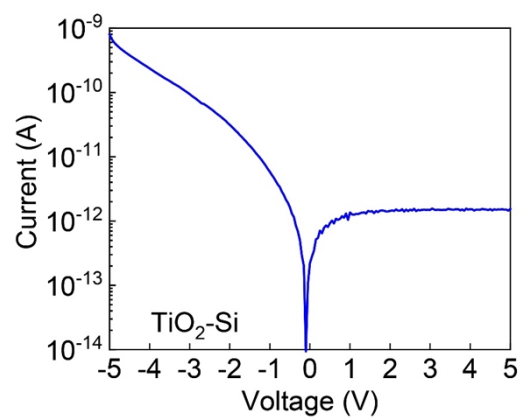
Supplementary Fig. 3 The read disturbance under 2 V/-2 V for HRS and LRS.



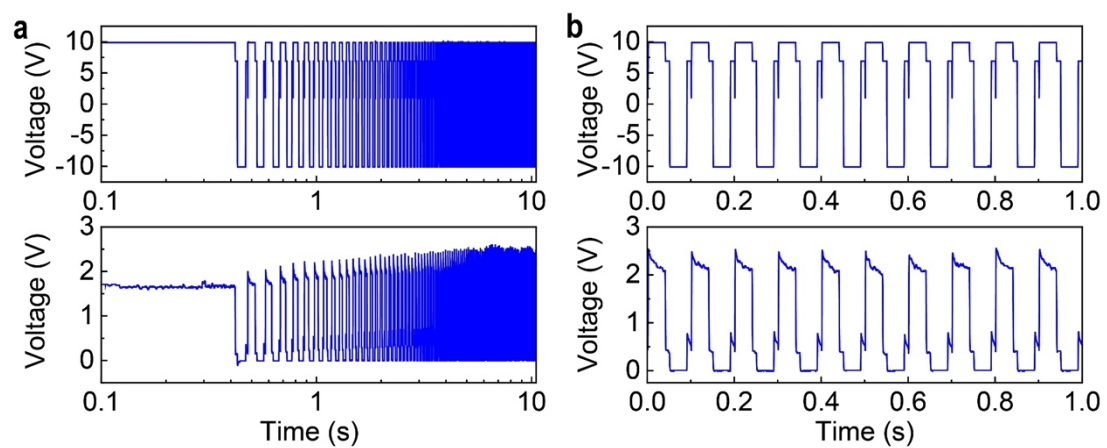
Supplementary Fig. 4 *I-V* characteristics of MXene-TiO₂-Si RRAMs with different thickness of TiO₂. (a) 2 nm, (b) 10 nm, (c) 15 nm.



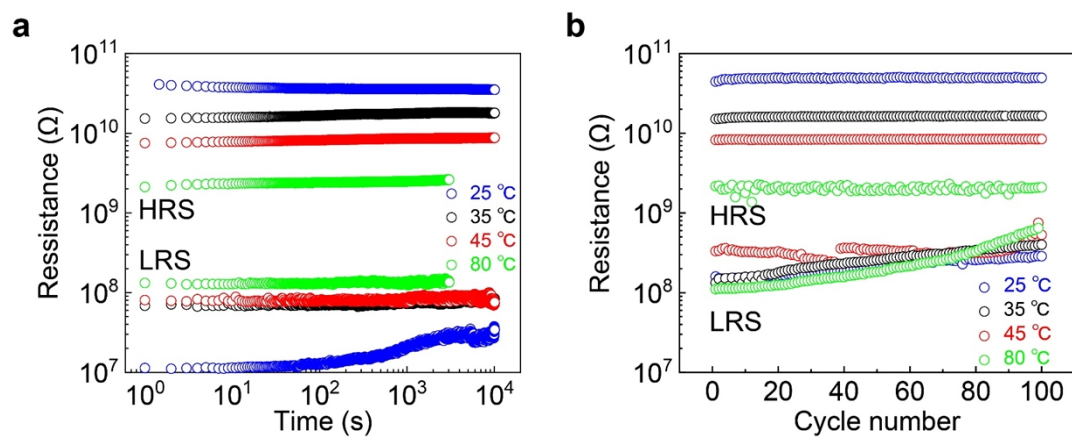
Supplementary Fig. 5 Typical I - V characteristics of MXene-TiO₂-Si RRAMs with different resistive area, indicating the bipolar SET and RESET processes. (a) $25 \mu\text{m}^2$, (b) $100 \mu\text{m}^2$, (c) $400 \mu\text{m}^2$, (d) $1600 \mu\text{m}^2$.



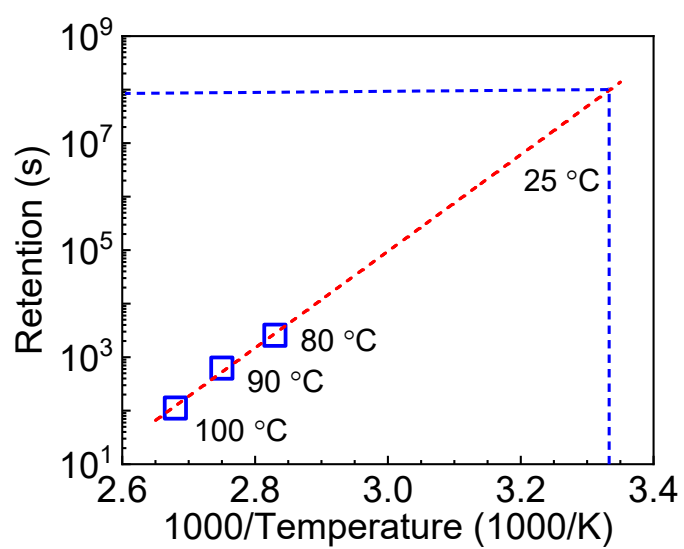
Supplementary Fig. 6 Typical *I-V* characteristic of $\text{TiO}_2\text{-Si}$ junction.



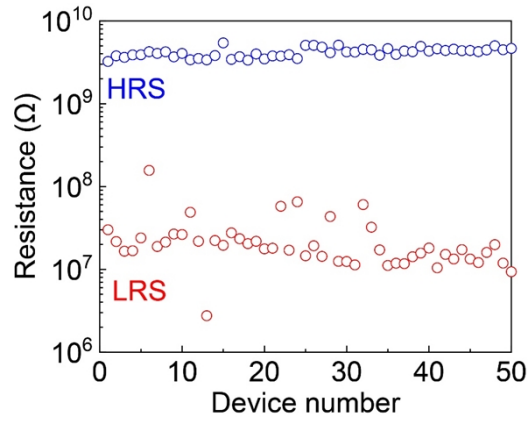
Supplementary Fig. 7 (a) Endurance test performed with more than 100 voltage sweep cycles in 10 s. (b) About 10 cycles in 1 s cut from (a).



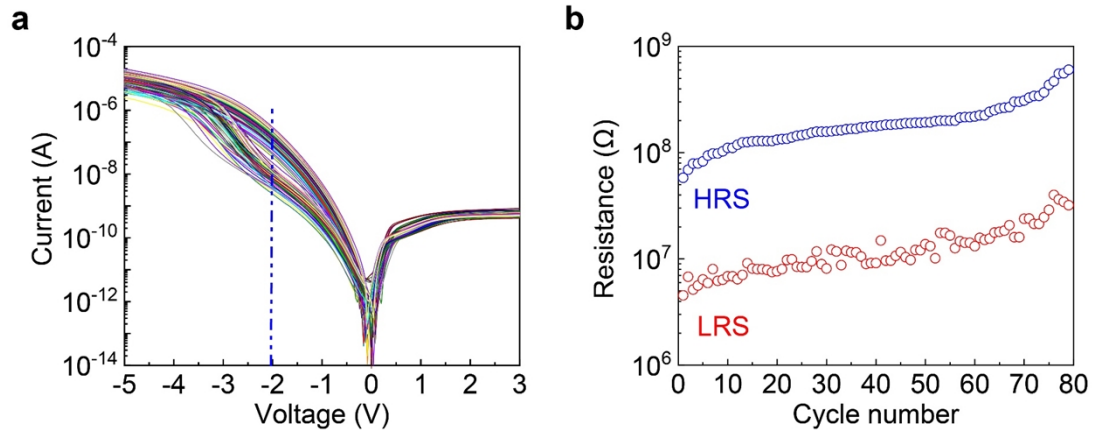
Supplementary Fig. 8 (a) Retention and (b) endurance characteristics at the different temperatures.



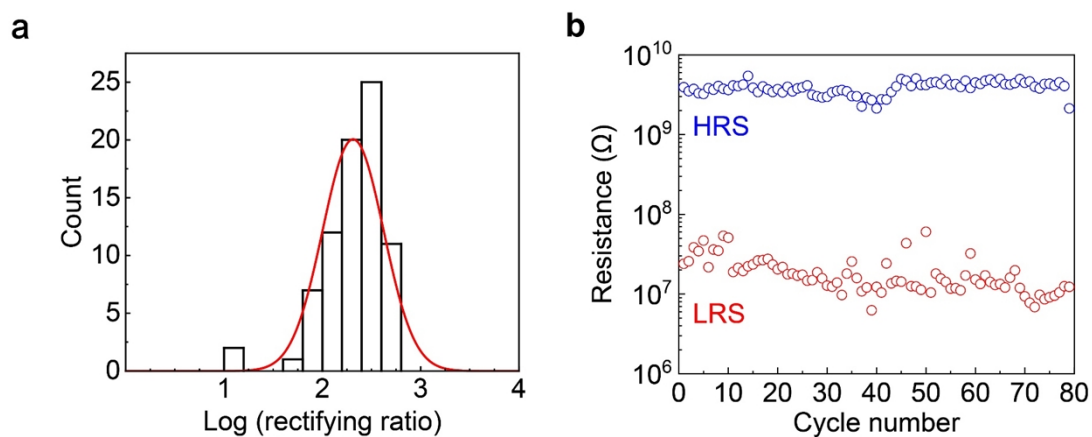
Supplementary Fig. 9 Temperature dependence of the retention time (s) follows the Arrhenius relation. Retention time at 25 °C are extrapolated from the linear fitting of measurement results (blue squares).



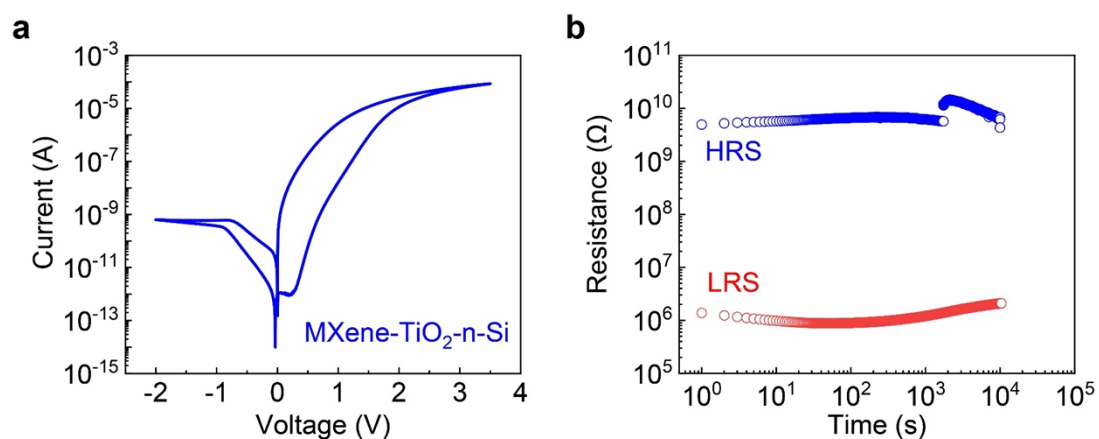
Supplementary Fig. 10 Device-to-device variation of HRS and LRS at the read voltage of 2 V, respectively.



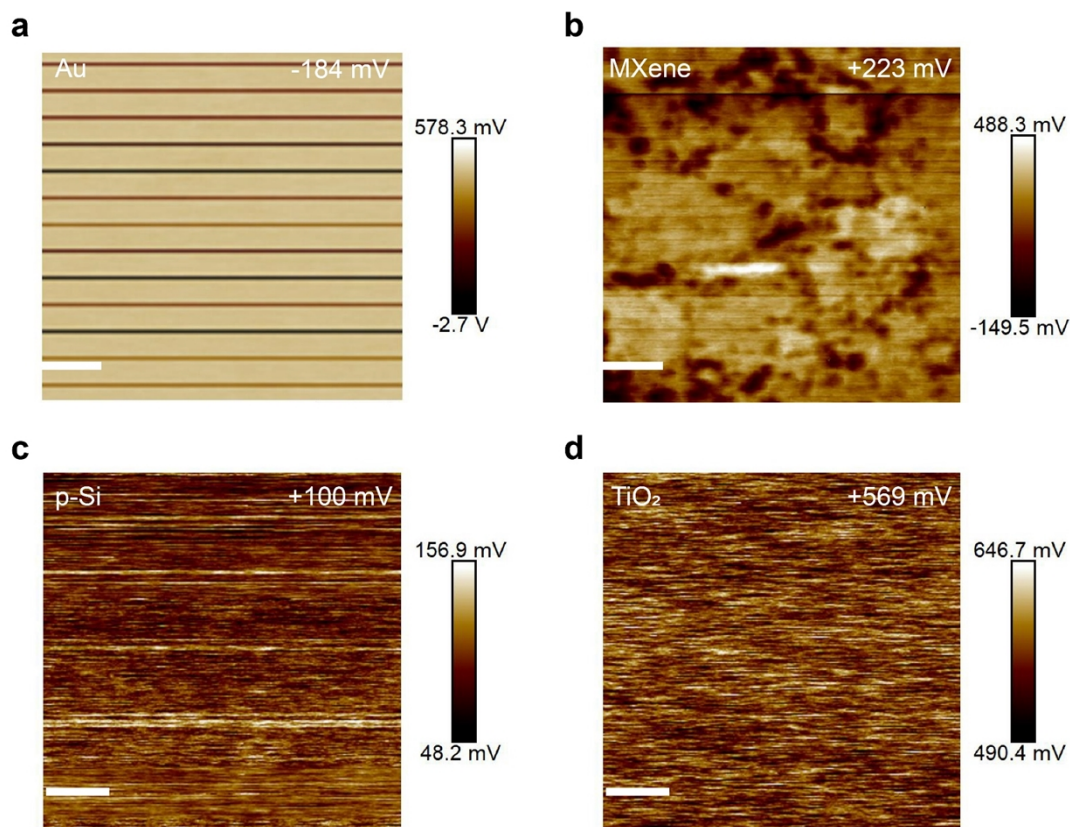
Supplementary Fig. 11 (a) The I - V characteristics of a single RRAM device with 80 cycles. (b) The extracted cycle-to-cycle distribution of HRS and LRS at 2 V read voltage. The resistance states can be also distinguished through the current on-off ratio more than 10



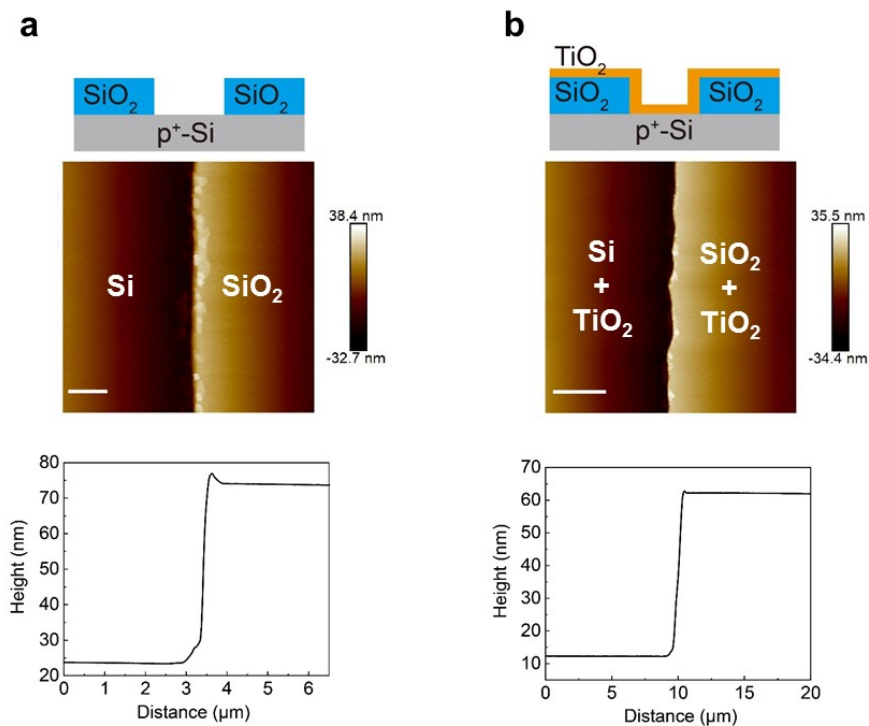
Supplementary Fig. 12 The statistical cycle-to-cycle variation of (a) rectifying ratio performed by a logarithmic operation and (b) HRS and LRS, respectively.



Supplementary Fig. 13 (a) Self-rectifying behavior and (b) retention characteristics of the MXene-TiO₂-n-Si.

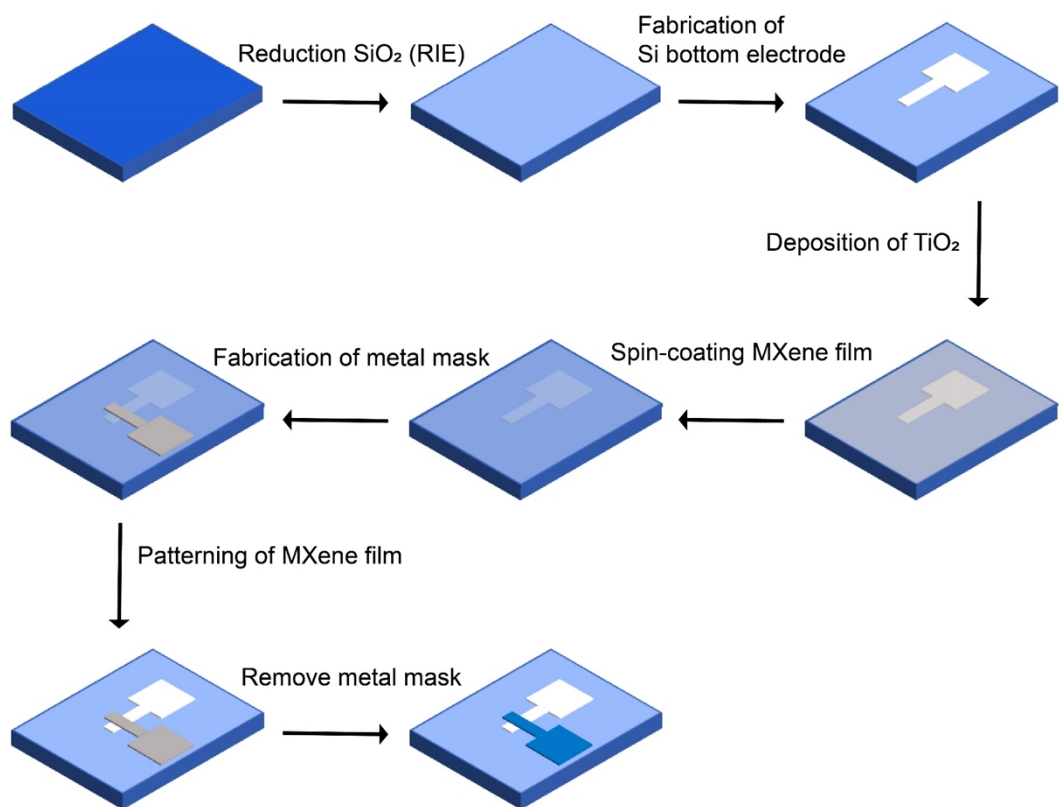


Supplementary Fig. 14 The Kelvin probe force microscopy (KPFM) potential map images and numerical analysis of (a) Au (scale bar: 840 nm), (b) MXene (scale bar: 1 μm), (c) $\text{p}^+\text{-Si}$ (scale bar: 1 μm) and (d) TiO_2 (scale bar: 1 μm). The potentials of Au, MXene, $\text{p}^+\text{-Si}$, and TiO_2 were -184 mV, $+223$ mV, $+100$ mV and $+569$ mV, respectively. The work function of Au is 5.2 eV. Therefore, the work function of MXene is $5.2 - 0.184 - 0.223 = 4.893$ eV, $\text{p}^+\text{-Si}$ is $5.2 - 0.184 - 0.1 = 5.016$ eV and TiO_2 is $5.2 - 0.184 - 0.569 = 5.547$ eV. (KPFM probe: SCM-PIT-V2, 0.01-0.025 Ohm-cm Antimony (n) doped Si).



Supplementary Fig. 15 The schematic, corresponding AFM and height of Si electrode

(a) before and (b) after 5-nm-TiO₂ deposited by ALD. Scale bar, 1 μm, 4 μm.



Supplementary Fig. 16 Fabrication flowchart of MXene-TiO₂-Si self-rectifying RRAMs.

Table S1. Performance comparison about TiO₂-based RRAM devices.

Structure	on/off ratio	rectifying ratio	Retention (s)	endurance
Ti/TiO ₂ /Pt ^[1]	10 ³	10 ⁵		1000
Cu/Ti/HfO ₂ /TiO ₂ /TiN ^[2]	3 × 10 ³			200
TaO _x /TiO ₂ /TaO _x ^[3]	10 ³		10 ⁴	10 ¹⁰
TiN/Ti/TiO _x /HfO _x /TiN ^[4]	10 ³		10 ⁴	
Pt/In ₂ Sn ₂ O ₃ /TiO ₂ /Pt ^[5]	160			40
TiN/TiO _x /Al ₂ O ₃ /IrO _x ^[6]	10	10	10 ⁵	1000
TiN/TiO _x /Al ₂ O ₃ /IrO _x ^[7]	30			10 ⁶
My work	10³	10³	10⁴	100

[1] Appl. Phys. Lett. 2020, 96, 262901.

[2] Advanced Electronic Materials 2020, 6 (9), 2000488□.

[3] ACS Nano 2012, 6, 9, 8166–8172.

[4] Appl. Phys. Lett. 2012, 101, 103506.

[5] Appl. Phys. Lett. 2008, 92, 162904.

[6] IEEE Transactions on Electron Devices 2018, 65 (3), 957-962□.

[7] ACS omega 2017, 2 (10), 6888-6895□.